POLITECNICO DI TORINO
Repository ISTITUZIONALE

Binary mixture in a 3-well ring: Characterization of amplication eects within the dynamical algebra so(2,3)

Original
Binary mixture in a 3-well ring: Characterization of amplication eects within the dynamical algebra so(2,3) / Giovannetti, M., Penna, V.. - In: PHYSICS LETTERS A. - ISSN 0375-9601. - STAMPA. - 599:(2026), pp. 1-10. [10.1016/j.physleta.2026.132255]

Availability:
This version is available at: 11583/3017013 since: 2026-10-26T11:24:00Z

Publisher:
Elsevier

Published
DOI:10.1016/j.physleta.2026.132255

Terms of use:

This article is made available under terms and conditions as specified in the corresponding bibliographic description in the repository

Publisher copyright

(Article begins on next page)

21 November 2026

Physics Letters A 599 (2026) 132255

Contents lists available at ScienceDirect

Physics Letters A

journal homepage: www.elsevier.com/locate/pla

Letter

Binary mixture in a 3-well ring: Characterization of amplification effects within the dynamical algebra so(2,3)

Martino Giovannetti [a], Vittorio Penna [b,*]

[a] Dipartimento di Scienze Matematiche, Politecnico di Torino, Corso Duca degli Abruzzi 24, I-10129 Torino, Italy
[b] Dipartimento di Scienza Applicata e Tecnologia, Politecnico di Torino, Corso Duca degli Abruzzi 24, I-10129 Torino, Italy

ARTICLE INFO

Communicated By Boris Malomed

Keywords:
Binary condensates
Dynamical algebra
Amplification effect

ABSTRACT

We investigate the quantum dynamics of a mixture formed by two interacting condensates in a ring geometry described by a Bose-Hubbard trimer. By implementing the Bogoliubov-approximation scheme we reduce the ring-trimer Hamiltonian to an effective quadratic form whose two-mode momentum operators constitute an algebra so(2,3). The latter, the dynamical algebra of the model, allows one to perform a complete diagonalization of the Hamiltonian, and to derive the exact time evolution of physical operators. While these aspects have been thoroughly studied in the stability regime of the ring trimer, the dynamical behavior in the instability regime has received little attention. To explore the latter, we violate the stability condition with a suitable change of the interspecies repulsion showing how this induces a spectral collapse, and drives the transition from purely-periodic oscillations of momentum-mode populations into an unstable dynamics featuring the populations' amplification. We thoroughly analyze the mechanism behind this macroscopic effect demonstrating how it smoothly emerges from the structural metamorphosis of the Hamiltonian and of its algebraic properties. We compare this effect with the parametric amplification of optical devices.

1. Introduction

Mixtures constituted by two bosonic species have proven to be a research ground of extraordinary interest because the unprecedented control of the inter-species interaction, and of the species densities combined with an adjustable trapping geometry has allowed the observation of a great variety of new dynamical behaviors and properties in a pristine environment fully dominated by quantum effects. An incomplete list of these includes the tunneling properties of a mixture in a double well [1], the formation of vortex-bright-soliton structures [2] and of exotic vortex lattices [3], the onset of persistent currents [4], the dynamics of two phase-separated components [5], the generation of quantum echo [6], and of intervortex bosonic Josephson supercurrents [7].

On the other hand, the study of single-component condensates trapped in small-size arrays of wells has attracted remarkable attention in the last three decades because such mesoscopic systems, described within the Bose-Hubbard (BH) picture [8], are able to trigger complex dynamical behaviors including the chaos onset, despite the relatively small number of wells and thus of bosonic space modes. This is the case, for example, of simplest possible array, the three-well system (trimer), thoroughly studied both in a purely-quantum perspective [9–12] and within semiclassical approaches [13–16] where chaotic behaviors crop up next to stable oscillations. This makes the trimer a paradigmatic model for this class of systems.

The inclusion of a second component considerably enriches the phenomenology of small arrays due to the inter-species interaction then leading to investigate the generation of elementary vortex excitations in a ring [17] and of maximum entanglement in mixtures [18], the competition between chaos and mixing [19], and the complex architecture of the ground-state phases [20] of a mixture. On the experimental front, the double-well trap has been realized in [21,22], while the design of the ring geometry for a multiwell array has been conceived more than twenty years ago in [23], and finds wide application within atomtronics [24,25]. Also, the trapping of bosonic mixtures has been achieved in three-dimensional optical lattices [26] and by means of hybrid traps [27].

The dynamics of binary mixtures, extensively studied through the mean-field approach for a double-well potential [28,29], triggers nontrivial behaviors when a third well [19] is introduced thus realizing a minimal yet highly nontrivial closed circuit supporting persistent currents and vortex-like excitations. For this reason, in this paper we consider a closed three-well trap hosting a two-species mixture, a system whose second-quantized version represents each species by means of a BH ring trimer. Particularly, we investigate how the algebraic properties

* Corresponding author.
E-mail address: vittorio.penna@polito.it (V. Penna).

https://doi.org/10.1016/j.physleta.2026.132255
Received 25 July 2026; Received in revised form 29 September 2026; Accepted 6 October 2026
Available online 10 October 2026
0375-9601/© 2026 The Author(s). Published by Elsevier B.V. This is an open access article under the CC BY license (http://creativecommons.org/licenses/by/4.0/).

of the Hamiltonian are closely related to the emergence of low-energy excitations and the possibility to trigger unstable behaviors.

We focus on the regime where both condensed species are superfluid and the ground state correspond to a uniform distribution across the ring lattice. This condition allows us to implement the Bogoliubov approximation scheme, moving from the space-mode picture to the momentum-mode picture, where collective excitations can be better described. Under the assumption that the zero-momentum modes are macroscopically occupied, the BH Hamiltonian of a generic L-site ring lattice decouples into many independent sub-Hamiltonians H_k, each one associated with a specific pair of momentum modes $\pm k$. As discussed in [17], each H_k is found to be an element of the Lie algebra so(2,3). The latter then represents the dynamical algebra [30,31] of the system, and its well-known properties can be used to investigate the spectral structure and the Heisenberg evolution of physical operators.

In particular, after revisiting the analytic derivation of the energy spectrum and of its characteristic frequencies in the stability domain of the parameter space, we investigate the transition to the unstable regime and the properties thereof. We show how the knowledge of the stability condition allows one to trigger the spectral collapse when the inter-species interaction overcomes the stability threshold. Particularly, the energy spectrum is shown to acquires a continuous component that can be seen as the signature of the dynamically-unstable regime [32]. To describe the dynamical transition, we calculate the Heisenberg time evolution of the momentum-mode populations showing that the periodic population oscillations of the stable regime mutate into an exponential diverging behavior that can be interpreted as an exponential growth of boson populations. In particular, we highlight the mechanism supporting such a macroscopic effect which, as in the case of the spectral collapse, completely depends on the algebraic properties of the Hamiltonian. Finally, thanks to the dynamical-algebra characterization of time evolution, we disclose how this effect is closely related to the amplification phenomenon occurring in well-known quantum-optics devices such as the (degenerate or non-degenerate) parametric amplifiers.

Our work is organized as follows. In Section 2, we introduce the ring-trimer Hamiltonian describing the binary mixture within the BH picture, and, by implementing the Bogoliubov approximation (revisited in Appendix A), we derive the quadratic Hamiltonian that allows one to identify the underlying dynamical algebra so(2, 3). The latter is discussed in Appendix B. In Section 3, we perform the diagonalization process giving the energy spectrum for both the stability and the instability regime. The exact time evolution of boson-mode populations in the stable phase is derived in Section 4, while the amplification effect of the unstable phase is discussed and compared to that of optical devices in Section 5 (see also Appendix C). Section 6 is devoted to the conclusions.

2. Momentum-mode picture and dynamical algebraic approach

The physical system under consideration consists of a binary mixture of two atomic condensates confined in a ring trimer. By incorporating an interspecies repulsive interaction, the many-body dynamics can be represented within the BH picture by the following second-quantized Hamiltonian:

$$H = H_A + H_B + W \sum_{i=1}^{3} N_i\, M_i, \tag{1}$$

where the third term describes the inter-species coupling by means of the local boson-number operators $N_i = A_i^\dagger A_i$ and $M_i = B_i^\dagger B_i$, while H_A and H_B represent the single-species BH Hamiltonians described by

$$H_C = \frac{U_c}{2} \sum_{i=1}^{3} C_i^{\dagger 2} C_i^2 - T_c \sum_{i=1}^{3} \left(C_{i+1}^\dagger C_i + C_i^\dagger C_{i+1} \right)$$

with $C = A, B$. In Hamiltonian (1), U_a and U_b characterize the intra-species repulsive strengths, T_a and T_b the hopping amplitudes for the two species, and parameter W accounts for the inter-species repulsion. Also, bosonic operators A_i, $A_i^\dagger$ and B_i, $B_i^\dagger$ satisfy the standard commutation relations

$$[A_j, A_i^\dagger] = [B_j, B_i^\dagger] = \delta_{j,i}, \quad [A_j, B_i^\dagger] = [A_j, B_i] = 0, \qquad j, i = 1, 2, 3.$$

The model features two conserved quantities

$$N = \sum_{i=i}^{3} N_i, \quad M = \sum_{i=i}^{3} M_i.$$

corresponding to the total particle numbers of the two species. To ensure that the system remains in a superfluid state and avoids Mott-insulator localization, we assume that the hopping terms T_a (T_b) dominate over the intra-species interactions U_a (U_b).

The property that, at zero temperature, both species macroscopically occupy their respective zero-momentum modes ($k = 0$), justifies the application of the Bogoliubov approximation. By transitioning to the momentum-mode picture where A_j, and B_j are expressed by means of the new modes a_k and b_k

$$A_j = \sum_{k=0}^{L-1} \frac{a_k}{\sqrt{L}} e^{+i\tilde{k}j}, \qquad B_j = \sum_{k=0}^{L-1} \frac{b_k}{\sqrt{L}} e^{+i\tilde{k}j}, \tag{2}$$

with $\tilde{k} = 2\pi k/L$ ($L = 3$ in the trimer case) and $k = 0, \pm 1$, and implementing the Bogoliubov procedure (see Appendix A) in which a_0 and b_0 are the macroscopically occupied modes, the resulting effective Hamiltonian for the ring trimer [17]

$$H = E_0 + H_1, \tag{3}$$

is composed by a constant energy term

$$E_0 = \frac{u_a}{2}(N-1) - 2NT_a + \frac{u_b}{2}(M-1) - 2MT_b + w\sqrt{NM} - (\gamma_a + \gamma_b)$$

and a term associated to the non-zero momentum modes

$$H_1 = 2(\gamma_a A_3 + \gamma_b B_3) + 2(u_a A_1 + u_b B_1) + 2w(K_1 + S_1), \tag{4}$$

where

$$X_1 = \frac{X_+ + X_-}{2}, \quad X_2 = \frac{X_+ - X_-}{2i}, \tag{5}$$

with $X_- = (X_+)^\dagger$, $X = A, B, K, S$ (note that operators X_2 will be utilized in the diagonalization process) and

$$A_+ = a_1^\dagger a_{-1}^\dagger, \qquad B_+ = b_1^\dagger b_{-1}^\dagger,$$
$$S_+ = a_1^\dagger b_1 + a_{-1}^\dagger b_{-1}, \qquad K_+ = a_{-1}^\dagger b_1^\dagger + a_1^\dagger b_{-1}^\dagger.$$

$$A_3 = \frac{n_1 + n_{-1} + 1}{2}, \qquad B_3 = \frac{m_1 + m_{-1} + 1}{2}. \tag{6}$$

Also, we define

$$\gamma_a = u_a + 3T_a, \quad \gamma_b = u_b + 3T_b,$$

obtained from Eq. (A.2) for $L = 3$, and

$$u_a = \frac{U_a N}{3}, \quad u_b = \frac{U_b M}{3}, \quad w = \frac{W\sqrt{NM}}{3}, \tag{7}$$

emerging from the Bogoliubov procedure. A fundamental property of the Hamiltonian (4) is that the operator set

$$\mathcal{A} = \{A_{1,2},\ B_{1,2},\ K_{1,2},\ S_{1,2},\ A_3,\ B_3\}$$

forms a closed structure under commutation. $\mathcal{A}$ defines the *dynamical algebra* of the system, a framework that proves highly efficient for determining conserved quantities, diagonalizing the Hamiltonian H_1, and predicting the time evolution of the physical operators of the system [30,32]. For our problem, $\mathcal{A}$ is identified as so(2,3) whose defining commutation relations are detailed in Appendix B. It is worth noting, in passing, the generality of this algebraic approach which easily extends to regimes of attractive intra-species interactions ($U_a, U_b < 0$). The formalism remains valid as long as the ratio $T_v/|U_v|$ is large enough to maintain the system in the superfluid phase.

3. Diagonalization of the model

The physical-state framework where the diagonalization of H_1 is performed, is the Hilbert space described by the Fock-state basis $\{|n_1, n_{-1}, m_1, m_{-1}\rangle\}$. The four quantum numbers $n_{\pm 1}$ and $m_{\pm 1}$ correspond to the numbers of bosons with momentum $p_k = \hbar\tilde{k}/a$ (a is the ring-lattice constant, and $\tilde{k} = 2\pi k/L$) with $k = \pm 1$ in either the condensed species. Note that, due to the closed trimer geometry, another quite natural way to interpret k is to refer this index to the angular momentum $\ell_k = rp_k = \hbar k$ where $r = La/2\pi$ is the ring radius.

In the particular case of twin species, where the assumptions $u_a = u_b =: u$, $T_a = T_b =: T$, and $N = M$ are made, the Hamiltonian H_1 becomes

$$H_1 = 2\gamma(A_3 + B_3) + 2u(A_1 + B_1) + 2w(K_1 + S_1), \tag{8}$$

with $\gamma = u + 3T$, and the diagonalization process is considerably simplified. Within the dynamical-algebra method, after recognizing that this Hamiltonian is an element (namely, a linear combination) of the generators of so(2,3), the diagonal form of H_1 is achieved by implementing a suitable unitary transformation $\mathcal{H}_1 = D^{-1}\, H_1\, D$, where D is an exponential operator belonging to the Lie group SO(2,3) generated by so(2,3). This transformation is found to be

$$D = e^{-i\phi S_2} e^{-i\theta_a A_2} e^{-i\theta_b B_2}.$$

Some good choices of angles ϕ, θ_a and θ_b lead to diagonalize H_1, that is, to get rid of those operators that are not diagonal in the Fock basis. By choosing:

$$\phi = \frac{\pi}{2}, \quad \tanh\theta_a = \frac{u+w}{\gamma+w}, \quad \tanh\theta_b = \frac{u-w}{\gamma-w}, \tag{9}$$

we obtain the diagonal Hamiltonian

$$\mathcal{H}_1 = D^{-1}\, H_1\, D = 2\hbar\Omega_a A_3 + 2\hbar\Omega_b B_3 \tag{10}$$

Operators A_3 and B_3, satisfying $[A_3, B_3] = 0$, are linear combination of number operators (see formulas (6)) and thus are, by construction, diagonal in the Fock basis. The new Hamiltonian $\mathcal{H}_1$ allows for a straightforward derivation of the energy eigenvalues, giving

$$E(n_1, n_{-1}, m_1, m_{-1}) = \frac{UN}{3}(N-3) + \frac{WN^2}{3} - (4N+6)T$$

$$+\hbar\Omega_a(n_1 + n_{-1} + 1) + \hbar\Omega_b(m_1 + m_{-1} + 1), \tag{11}$$

where the constant E_0 has been written explicitly, and the characteristic frequencies Ω_a, Ω_b read

$$\Omega_a = \frac{1}{\hbar}\sqrt{2TUN\left(1 + \frac{9T}{2UN} + \frac{W}{U}\right)}, \tag{12}$$

$$\Omega_b = \frac{1}{\hbar}\sqrt{2TUN\left(1 + \frac{9T}{2UN} - \frac{W}{U}\right)}. \tag{13}$$

An important property of spectrum (11) is its discrete character, a circumstance due to the fact that A_3 and B_3 are linear combinations of number operators and thus feature a discrete spectrum. This allows to identify A_3 and B_3 as the compact operators of so(2,3). Such property reflects, at the quantum-mechanical level, on the stability of the system because any energy variation can be realized only exchanging finite energy quanta with some external system. Additionally, the spectrum structure can be easily shown to generate a time evolution of (the expectation value of) physical operators that essentially features an oscillatory behavior.

Nevertheless, these nice properties can be violated by suitable choices of the model parameters that suppress the real-valued character of the present spectrum. As is well known, such an effect is anticipated by the spectrum collapse and is accompanied by the emergence of a totally different dynamical scenario representing the transition to the unstable regime.

3.1. Instability regime: diagonalization and spectral collapse

A fundamental information relevant to the previous diagonalization scheme emerges when we analyze the parameter space defined by (U, T, W, N). By inspecting the definitions of the characteristic frequencies (12) and (13), it becomes evident that while Ω_a is strictly real for physically meaningful parameters, Ω_b can assume purely imaginary values. In particular it becomes imaginary within a specific region of the parameter space, defined as

$$\Gamma = \left\{(U, T, W, N) : \frac{W}{U} > \chi = 1 + \frac{9T}{2UN}\right\}. \tag{14}$$

When the ratio W/U violates the upper bound χ, the energy spectrum collapses, signaling the onset of dynamical instability [32–34]. In this regime, the system enters an unstable phase, and the diagonalization procedure previously outlined loses its physical validity.

For parameters' choices falling in the instability region Γ, the correct description of the quantum dynamics requires that the diagonalization strategy is substantially revised since the apparently harmless change of the coefficients of the so(2,3) generators forming H_1 remarkably modifies the algebraic structure of the resulting diagonal Hamiltonian. To restore the real-valued character of the transformed Hamiltonian, we must modify the unitary transformation determining the diagonalization of the Hamiltonian. Unlike transformation D, leading to Hamiltonian (10) formed by two compact operators A_3 and B_3, the new transformation S maps the Hamiltonian onto a non-compact generator, specifically B_1, while retaining the well-behaved compact generator A_3. S, exhibiting the same structure of D, is defined by imposing a different pair of constraints on the generalized rotation angles

$$\tanh\theta_a = \frac{u+w}{\gamma+w}, \qquad \tanh\tilde{\theta}_b = \frac{w-\gamma}{w-u}. \tag{15}$$

so that, unlike Ω_a, the new characteristic frequency $\tilde{\Omega}_b$ takes the form

$$\tilde{\Omega}_b = \frac{1}{\hbar}\sqrt{2TUN\left(\frac{W}{U} - \frac{9T}{2UN} - 1\right)}. \tag{16}$$

Crucially, when the trimer parameters satisfy the condition (14) defining Γ, the quantity below the square root of $\tilde{\Omega}_b$ is strictly positive, guaranteeing that both Ω_a and $\tilde{\Omega}_b$ are real numbers.

Thanks to conditions (15) the transformation S provides the diagonal Hamiltonian

$$\mathcal{H}_1' = S^{-1} H_1\, S = 2\hbar\Omega_a A_3 - 2\hbar\tilde{\Omega}_b B_1. \tag{17}$$

Unlike A_3, the operator B_1 (which, however, commutes with A_3) is not diagonal in the standard Fock basis. Within the algebra so(2,3), in fact, operator B_1 is recognized to form, together with operators B_3 and B_2, a subalgebra su(1,1)

$$[B_1, B_2] = -iB_3, \quad [B_2, B_3] = iB_1, \quad [B_3, B_1] = iB_2,$$

as shown by the commutator list of Appendix B. While B_3 represents a compact generator of su(1,1), a features entailing that (similar to A_3) it exhibits a discrete spectrum, both B_1 and B_2, in virtue of their non-compact character, can be shown to be associated with a continuous spectrum. In particular, the distinctive trait of B_1, and B_2 is that they are diagonalized by the Lindblad-Nagel states [35] characterized by continuous eigenvalues belonging to $\mathbb{R}$. Consequently, in the present case, the energy spectrum of this regime is

$$E(\{n_1, n_{-1}, \eta\}) = \frac{UN}{3}(N-3) + \frac{WN^2}{3} - 4NT$$

$$-6T + \hbar\Omega_a(n_1 + n_{-1} + 1) - 2\hbar\tilde{\Omega}_b\eta, \qquad \eta \in \mathbb{R}, \tag{18}$$

showing how the emergence of a continuous component in the spectrum implies the loss of the stability characteristic of the discrete energy spectrum. Any infinitesimal energy perturbations, in fact, is able to trigger the transitions to different energy eigenstates. Then, a distinctive feature of the transition to the unstable regime is that, within Γ, the energy spectrum acquires a continuous component caused by the operator B_1

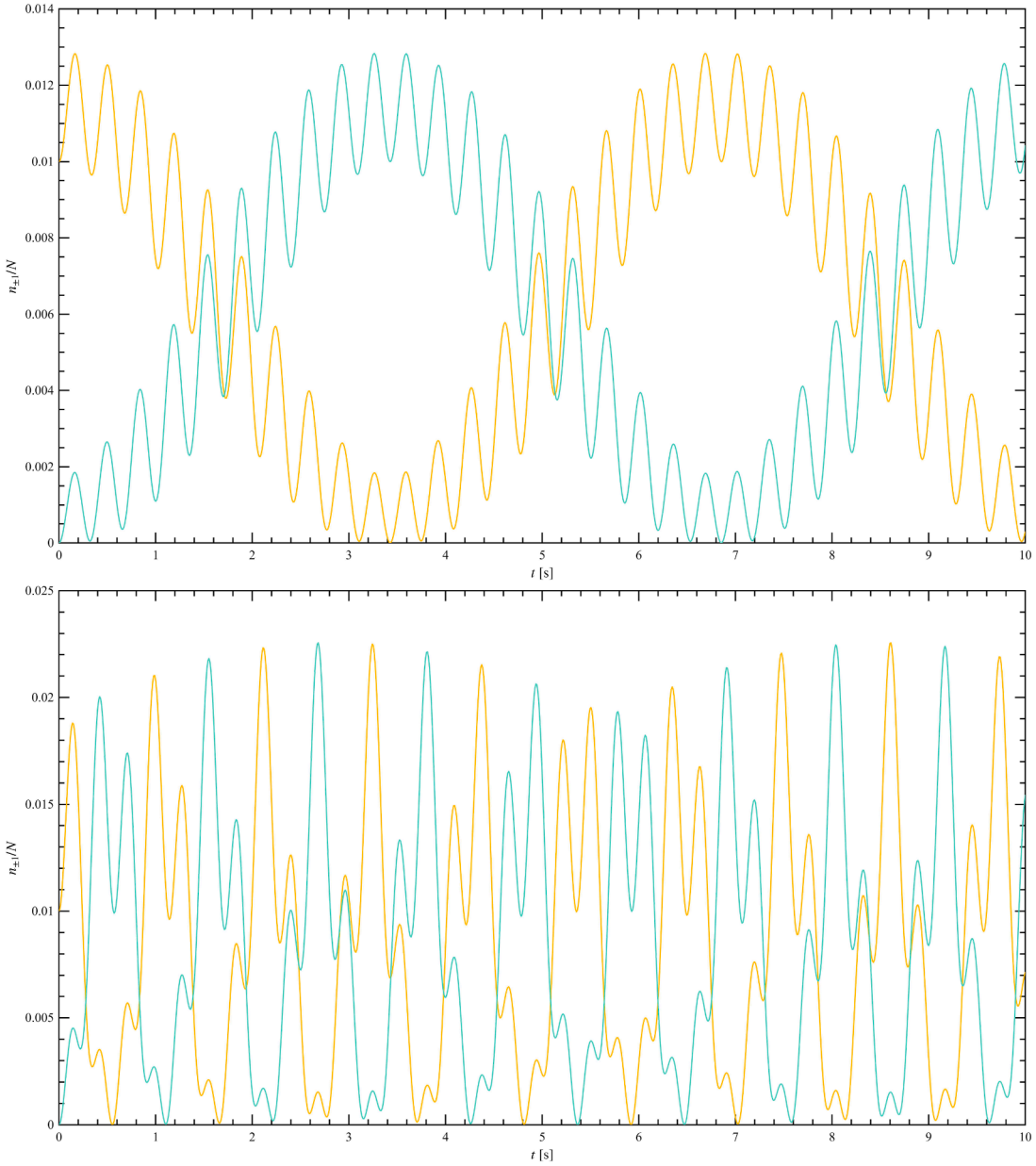


Fig. 1. Population dynamics for $T = 2$, $N = 1000$, and $U = 0.01$, with initial conditions $n_{-1}(0) = m_1(0) = 10$ and $m_{-1}(0) = n_1(0) = 0$. The yellow and blue lines represent the n_{-1} and n_1 populations, respectively. The top panel illustrates a weakly interacting regime ($W/U = 0.4$), while the bottom panel depicts a strongly interacting case ($W/U = 1.2$). Notably, both configurations lie within the stable regime, exhibiting oscillatory behavior without exponential growth.

in Hamiltonian (17). These behavior can be interpreted as a precursor, in a few-well scenario, of the symmetry-breaking transition with phase separation observed in mixtures characterized by strong enough interspecies interactions with $W/U > 1$ (see, e.g., [20,36]). The same inequality emerges from definition (14) in the large-N limit.

4. Time evolution in the stable regime

To fully characterize the system behavior across the different dynamical regimes, we investigate the time evolution of relevant physical observables. We focus on the expectation value of the number operator for the $k = 1$ mode, $\langle \hat{n}_1 \rangle_t$, which physically represents the first excited momentum state corresponding to a quantized particle circulation along the ring or, equivalently, to the angular-momentum state $\ell_1 = \hbar$ (elementary vortex excitation).

To calculate this quantity, we employ the well-known semiclassical Weyl-Heisenberg coherent states (see, for example, Ref. [37])

$$|\alpha_k\rangle = e^{-\frac{|\alpha_k|^2}{2}} \sum_{n=0}^{\infty} \frac{\alpha_k^n}{\sqrt{n!}} |n\rangle, \tag{19}$$

where $k = \pm 1$, satisfying the defining equation $a_k|\alpha_k\rangle = \alpha_k|\alpha_k\rangle$ with $\alpha_k \in \mathbb{C}$. Similar states $|\beta_k\rangle$ such that $b_k|\beta_k\rangle = \beta_k|\beta_k\rangle$ can be defined for the modes b_k. By assuming that the initial state of the system is the product coherent state $|\xi\rangle = |\alpha_1\rangle|\alpha_{-1}\rangle|\beta_1\rangle|\beta_{-1}\rangle$, the time evolution of the population $\langle \hat{n}_1 \rangle_t$ is described by

$$\langle \hat{n}_1 \rangle_t = \langle a_1^\dagger a_1 \rangle_t = \langle \xi | P_t^\dagger a_1^\dagger a_1 P_t | \xi \rangle,$$

where $P_t = e^{-i\frac{t}{\hbar}H_1}$ is the time-evolution operator such that $\hat{P}_t|\xi\rangle$ is a solution to the Schrödinger equation for the initial state $|\xi\rangle$. The explicit evaluation of the time-evolved operator

$$\hat{n}_1(t) = P_t^\dagger a_1^\dagger a_1 P_t \tag{20}$$

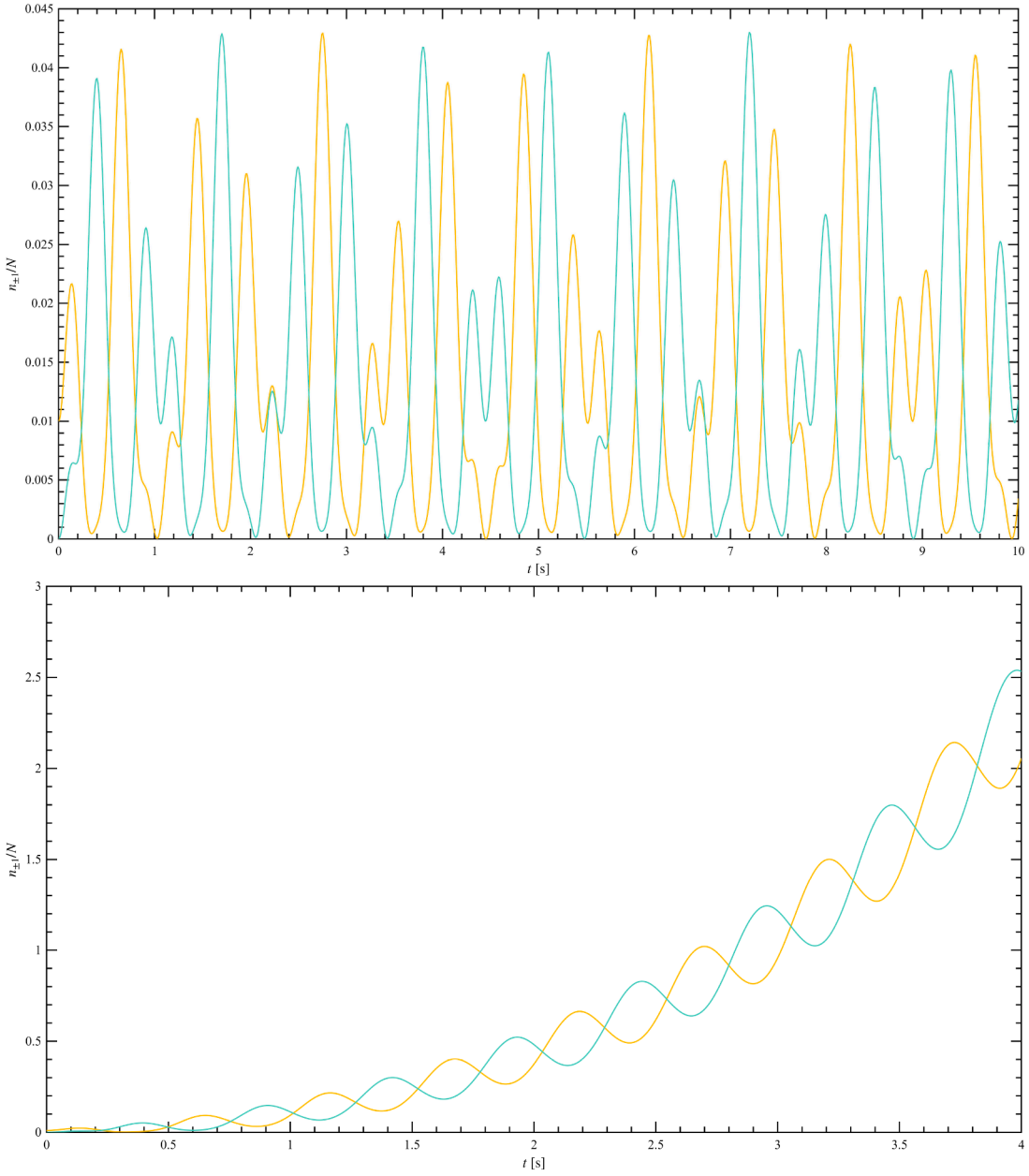


Fig. 2. Population dynamics for $T = 2$, $N = 1000$, and $U = 0.01$, with initial conditions $n_{-1}(0) = m_1(0) = 10$ and $m_{-1}(0) = n_1(0) = 0$. The yellow and blue lines represent the n_{-1} and n_1 populations, respectively. The top panel illustrates a strong-interaction case ($W/U = 1.7$) inside the stability region, while the bottom panel ($W/U = 1.902$) depicts the onset in the instability region of the exponential growth corresponding to the amplification effect.

within the Heisenberg picture strongly depends on the dynamical regime in which the Hamiltonian is diagonalized.

4.1. Population dynamics

In this subsection, we evaluate the time behavior characterizing the expectation value $\langle \hat{n}_1 \rangle_t$. Our goal is to highlight the oscillatory (non diverging) behavior of the boson population when the system parameters lie outside the unstable region Γ. This will be subsequently compared with the behavior of the same quantity in the unstable regime.

After recalling that the diagonal Hamiltonian $\mathcal{H}_1$ described by (10) is related to the original Hamiltonian by $H_1 = D\mathcal{H}_1 D^\dagger$, the propagator can be recast into the form

$$P_t = De^{-i\frac{t}{\hbar}\mathcal{H}_1} D^\dagger. \tag{21}$$

To highlight the dynamical behavior in the stable regime (note that the same scheme can be extended to the unstable regime), we adopt the Heisenberg-picture viewpoint and calculate the evolution of the number operator [38]

$$\hat{n}_1(t) = P_t^\dagger a_1^\dagger a_1 P_t = \left(De^{i\frac{t}{\hbar}\mathcal{H}_1} D^\dagger\right) a_1^\dagger a_1 \left(De^{-i\frac{t}{\hbar}\mathcal{H}_1} D^\dagger\right).$$

Since P_t is a unitary operator, the identity resolution $P_t P_t^\dagger = \mathbb{I}$ leads to the more tractable form

$$\hat{n}_1(t) = \left(P_t^\dagger a_1 P_t\right)^\dagger \left(P_t^\dagger a_1 P_t\right) = R^\dagger R.$$

The explicit expression for the time-evolved operator R is obtained by implementing the unitary transformation P_t on the boson mode a_1. One finds

$$R = P_t^\dagger a_1 P_t = C_{a,1} a_1 + C_{a,2} a_{-1}^\dagger + C_{b,1} b_1 + C_{b,2} b_{-1}^\dagger.$$

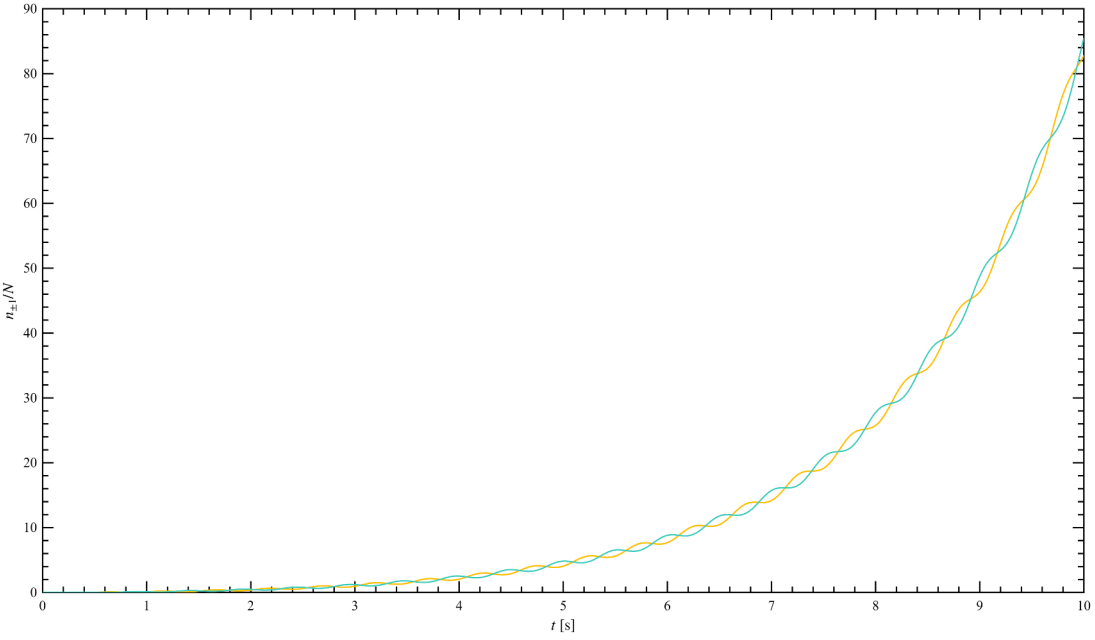


Fig. 3. Population dynamics for $T = 2$, $N = 1000$, $U = 0.01$, $W/U = 1.902$, with initial conditions $n_{-1}(0) = m_1(0) = 10$ and $m_{-1}(0) = n_1(0) = 0$. The choice of parameters lie in unstable domain Γ. A large (unphysical) time interval is used to show the exponential character of the population growth.

whose time-dependent coefficients are defined as

$$2C_{a,1}(t) = \cos\tau_a - i\mathrm{ch}\theta_a \sin\tau_a + \cos\tau_b - i\mathrm{ch}\theta_b \sin\tau_b, \tag{22}$$

$$2C_{a,2}(t) = -i\mathrm{sh}\theta_a \sin\tau_a - i\mathrm{sh}\theta_b \sin\tau_b, \tag{23}$$

$$2C_{b,1}(t) = \cos\tau_a - i\mathrm{ch}\theta_a \sin\tau_a - \cos\tau_b + i\mathrm{ch}\theta_b \sin\tau_b, \tag{24}$$

$$2C_{b,2}(t) = -i\mathrm{sh}\theta_a \sin\tau_a + i\mathrm{sh}\theta_b \sin\tau_b, \tag{25}$$

where the dimensionless variables $\tau_a \equiv t\Omega_a$ and $\tau_b \equiv t\Omega_b$ encapsulate the entire time dependence of the system.

In the light of this, by evaluating the expectation value over the initial coherent state, $\langle \hat{n}_1 \rangle_t = \langle \xi | R^\dagger R | \xi \rangle$, we obtain the explicit time evolution (the time is implied in sysmbols (22–25)) of the boson population

$$\langle \hat{n}_1 \rangle_t = |C_{a,2}|^2 + |C_{b,2}|^2 + \left| C_{a,1}\alpha_1 + C_{a,2}\alpha^*_{-1} + C_{b,1}\beta_1 + C_{b,2}\beta^*_{-1} \right|^2, \tag{26}$$

where the parameter-independent term $C_0(t) = |C_{a,2}|^2 + |C_{b,2}|^2$ represents the spontaneous creation of particle pairs from the vacuum state ($\alpha_{\pm 1} = \beta_{\pm 1} = 0$).

As evident from the explicit definitions of the coefficients C, the dimensionless time variables τ_a and τ_b appear exclusively as arguments of trigonometric functions (sines and cosines). Consequently, despite the analytic complexity of its expression, the time-dependent average population $\langle \hat{n}_1 \rangle_t$ exhibits regular, periodic oscillations characterized by frequencies Ω_a and Ω_b. Similar calculations can be effected for $\hat{n}_{-1}$ and $\hat{m}_{\pm 1}$ which provide analytic expressions similar to formula (26). This purely oscillatory dynamics is illustrated in Fig. 1 for the populations $\langle \hat{m}_1 \rangle_t$ and $\langle \hat{n}_{-1} \rangle_t$. It represents the hallmark of the stable regime, physically corresponding to a bounded, coherent exchange of particles between the modes in the absence of any macroscopic amplification.

5. Amplification effect in the instability region Γ

With an analogous procedure, we can investigate the behavior of the boson population when the parameter choice falls within the instability region Γ. In this regime, the diagonalized Hamiltonian is denoted by $\mathcal{H}_1{}'$.

After recalling that $H_1 = S\mathcal{H}_1{}'S^\dagger$, with S the unitary transformation that diagonalizes the system, the time propagator takes the form

$$P_t = Se^{-i\frac{t}{\hbar}\mathcal{H}_1{}'}S^\dagger. \tag{27}$$

By operating once again in the Heisenberg picture, the time evolution of the number operator takes the form

$$\hat{n}_1(t) = P_t^\dagger a_1^\dagger a_1 P_t = \left(Se^{i\frac{t}{\hbar}\mathcal{H}_1{}'}S^\dagger\right) a_1^\dagger a_1 \left(Se^{-i\frac{t}{\hbar}\mathcal{H}_1{}'}S^\dagger\right)$$

$$= \left(P_t^\dagger a_1 P_t\right)^\dagger \left(P_t^\dagger a_1 P_t\right) = \tilde{R}^\dagger \tilde{R}. \tag{28}$$

The time-evolved operator $\tilde{R}$ can be expressed as a linear combination of the fundamental momentum modes

$$\tilde{R} = \tilde{C}_{a,1}a_1 + \tilde{C}_{a,2}a^\dagger_{-1} + \tilde{C}_{b,1}b_1 + \tilde{C}_{b,2}b^\dagger_{-1}. \tag{29}$$

The explicit coefficients governing the dynamics in the unstable regime take the following symmetric form

$$2\tilde{C}_{a,1}(t) = \cos\tau_a - i\mathrm{ch}\theta_a \sin\tau_a + \mathrm{ch}\tau_b + i\mathrm{sh}\tilde{\theta}_b \mathrm{sh}\tilde{\tau}_b, \tag{30}$$

$$2\tilde{C}_{a,2}(t) = -i\mathrm{sh}\theta_a \sin\tau_a + i\mathrm{ch}\tilde{\theta}_b \mathrm{sh}\tilde{\tau}_b, \tag{31}$$

$$2\tilde{C}_{b,1}(t) = \cos\tau_a - i\mathrm{ch}\theta_a \sin\tau_a - \mathrm{ch}\tilde{\tau}_b - i\mathrm{sh}\tilde{\theta}_b \mathrm{sh}\tilde{\tau}_b, \tag{32}$$

$$2\tilde{C}_{b,2}(t) = -i\mathrm{sh}\theta_a \sin\tau_a - i\mathrm{ch}\tilde{\theta}_b \mathrm{sh}\tilde{\tau}_b. \tag{33}$$

Here, the dimensionless time variables are defined as $\tau_a \equiv t\Omega_a$ and $\tilde{\tau}_b \equiv t\tilde{\Omega}_b$.

By taking the expectation value of the time-evolved number operator over the initial coherent state $|\xi\rangle$, we obtain the exact time evolution of the boson population in the unstable regime

$$n_1(t) = \langle \hat{n}_1 \rangle_t = |\tilde{C}_{a,2}|^2 + |\tilde{C}_{b,2}|^2 + \left| \tilde{C}_{a,1}\alpha_1 + \tilde{C}_{a,2}\alpha^*_{-1} + \tilde{C}_{b,1}\beta_1 + \tilde{C}_{b,2}\beta^*_{-1} \right|^2, \tag{34}$$

where $C_0(t) = |\tilde{C}_{a,2}|^2 + |\tilde{C}_{b,2}|^2$ represent the effect of the vacuum state. A crucial physical distinction then emerges when comparing these results to the stable case. While the stable-regime coefficients (22)–(25) contribute with purely-periodic oscillations governed by $\sin(t\Omega_a)$, and $\cos(t\Omega_a)$, the unstable-regime coefficients (30)–(33) always include hyperbolic functions such as $\sinh\tilde{\tau}_b$, and $\cosh\tilde{\tau}_b$ combined with other oscillatory terms. This structural difference completely alters the underlying

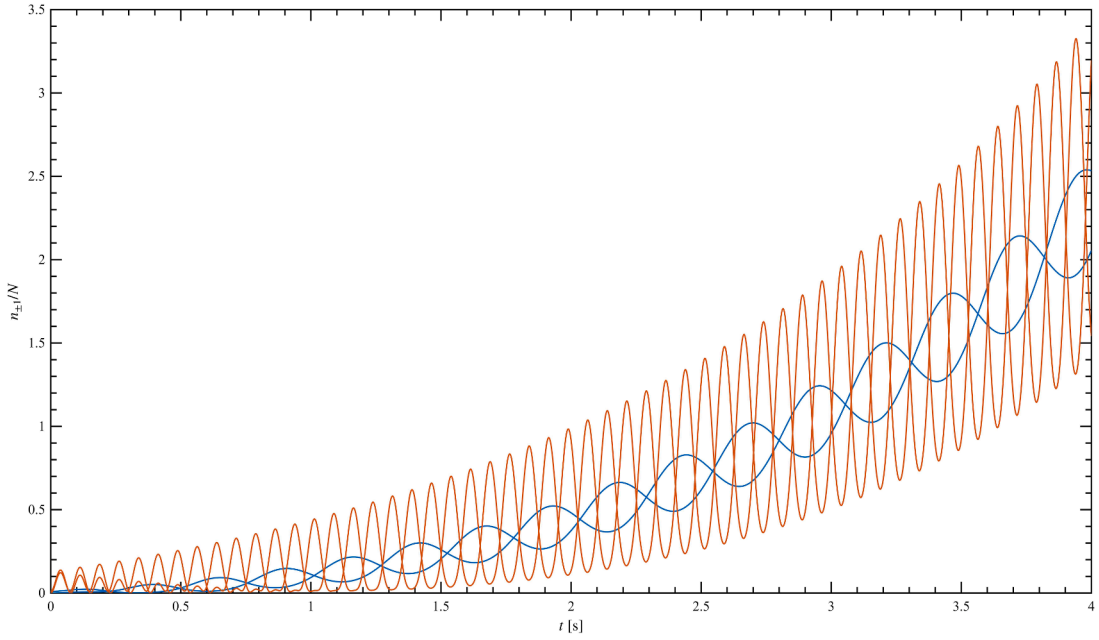


Fig. 4. Population dynamics of $n_{\pm 1}(t)$ for $T = 2$, $N = 1000$, with initial conditions $n_{\pm 1}(0) = 10$. When $\delta = 0$, small oscillations (blue plots) of $n_{\pm 1}(t)$ are superimposed to the exponential growth for $U = 0.01$, $W/U = 1.902$. The case $\delta = 0.2$ exhibits the same growth but larger oscillations (red plots) of $n_{\pm 1}(t)$ take place due to the shifts $U' = U + \delta$, $W' = W + \delta$.

dynamics: rather than pure bounded oscillations, the population exhibits an exponentially diverging behavior over time. This exponential growth effectively corresponds to the amplification of the population $n_1(t)$, and represents the macroscopic signature of the parametric instability characterizing the domain Γ. For time t large enough, formulas (30)–(33) exhibit the same time behavior clearly showing the amplification effect

$$n_1(t) = \langle \hat{n}_1 \rangle_t \simeq \text{const} \times e^{2t\tilde{\Omega}_b}. \tag{35}$$

The calculation of $n_{-1}(t)$ and $m_{\pm 1}(t)$ can be shown to reveal the same behaviors found for $n_1(t)$ in both the stable and the unstable regime. Then, in the latter case the dynamics exhibits a collective increasing of all the boson populations of the excited states. Fig. 2 shows the transition from the stability (upper panel) to the instability (lower panel) regime obtained by varying the effective interaction W/U. Fig. 3 is introduced, for illustrative purposes, to emphasize the exponential growth on a large (unphysical) time interval. Formulas (12) and (16), rewritten in the form

$$\Omega_a = \frac{1}{\hbar}\sqrt{2TN(W + U + \sigma)}, \quad \sigma = \frac{9T}{2N},$$
$$\tilde{\Omega}_b = \frac{1}{\hbar}\sqrt{2TUN(W - U - \sigma)},$$

demonstrate how the exponential growth is essentially characterized by $W - U$ while the oscillatory behavior depends on $W + U$ (note that σ is negligible for N large enough). The consequence of this feature is described in Fig. 4 where the exponential growth is shown for $W' = W + \delta$, and $U' = U + \delta$ with both $\delta = 0$ and $\delta = 0.2$. While the exponential trend is not affected by the shift of W and U, the oscillatory behavior significantly increases its amplitude.

The physical interpretation of this instability, which manifests itself with a diverging exponential behavior, naturally emerges from the comparison with the amplification effect characterizing the parametric amplifiers of quantum optics [39,40]. The latter is revisited in Appendix C where, interestingly, the same algebraic properties of Hamiltonian (17) in the instability regime (namely, the presence of a non-compact operator) are shown to support the occurrence of the amplification effect.

An important remark concerns the validity of this amplification effect. While the predictions based on the previous calculations suggest that the population growth could be unlimited, the Bogoliubov scenario discussed in Section 2 to get Hamiltonian (3), reminds us that the zero-momentum modes are associated to a maximum boson number of the order of N. The zero-momentum populations of the two species $n_0 \simeq N_a = N$ and $m_0 \simeq N_b = N$, representing the boson reservoirs, are thus large but finite meaning that the amplification effect takes place on a finite time interval. This is the same mechanism of the parametric-amplifier models of quantum optics, where the pump mode, associated with a large number of photons (and described in a semiclassical picture), supports the generation of an increasing number of photons (through two-photon processes) on a finite time interval. In our model, when $n_1(t)$ (and the populations of the other modes) becomes comparable with the value N the model loses its physical significance.

6. Conclusion

We studied the instability regime characterizing the dynamics of a binary mixture confined in a ring lattice. For the sake of simplicity, we considered the model Hamiltonian, represented in the BH picture, in the case of the minimal closed geometry, the 3-well ring. After reducing the trimer Hamiltonian to a quadratic form through the Bogoliubov approximation, we explored its instability regime by applying the dynamical-algebra approach.

The diagonalization process revealed that the diagonal Hamiltonian of the stable regime is formed by the compact generators of so(2,3), a circumstance that induced the discrete structure of the energy spectrum (11) characterized by frequencies (12) and (13). The latter frequency allowed us to identify, in the space of model parameters, the boundary separating the stability domain from the instability domain Γ. Inside Γ, the diagonalization process reveals significant changes of the structure of the diagonal Hamiltonian. The latter, in fact, exhibits a non-compact operator of so(2,3) representing the dramatic metamorphosis of the energy spectrum into the new form (18) including a continuous component. This is the hallmark of the dynamical transition to the instability regime which is anticipated by the reduction of the energy-level distance and culminates with the spectral collapse ($\Omega_b \to 0$) in Eq. (11) when approaching the domain Γ (this occurs, for example, when W/U tends to the critical value χ from below).

While the compact character of the diagonal Hamiltonian in the stability regime reflects on a time evolution of momentum-mode

populations by determining the periodic oscillatory behavior derived in Section 4, the instability regime, where the diagonal Hamiltonian (17) now includes a non-compact operator of so(2,3), features the emergence of momentum-mode populations with a diverging exponential behavior, discussed in Section 5, which, for times large enough, dominate the populations' evolution and can be seen as an amplification effect.

The comparison with the amplification effect of the photon number observed in the (either degenerate or non-degenerate) parametric amplifiers of quantum optics reveals how the mechanism causing the exponantial growth is the same. In particular, the root of this effect is related to the algebraic properties of the model Hamiltonian, and, more specifically, consists in the dramatic change of the diagonal Hamiltonian (controlled thorough the model parameters) when a non-compact generator of the dynamical algebra crops up in place of a compact one. The Heisenberg picture where propagators (21) and (27) depend on $\mathcal{H}_1$ (stability regime) and $\mathcal{H}_1'$ (instability regime), respectively, clearly shows how the algebraic character of such Hamiltonians determines the presence of time-dependent cosine or sine-like terms in (26) or their replacement with time-dependent hyperbolic terms in (34) causing the amplification effect.

Concluding, the algebraic properties of the Hamiltonian represent the tool for interpreting the exponential growth of the instability regime, and for revealing the mechanism governing such an effect. Among various aspects, future work will be developed in two directions. First, it is interesting to study mixtures where, instead of twin condensates, each components exhibit independent parameters. This causes a more complex structure of the parameter space and of the diagonalization process, involving, in parallel, the possibility to discover different routes to trigger amplification effects. Second, a promising extension of the analysis effected in this paper should be viable for Bose-Hubbard-like systems (a large class of these, for example, is represented by atomtronics devices [25]) where the dynamical-algebra methods can be applied and the dynamics exhibits instability regimes.

CRediT authorship contribution statement

Martino Giovannetti: Writing – original draft, Validation, Formal analysis, Conceptualization; **Vittorio Penna:** Writing – review & editing, Validation, Supervision, Formal analysis, Conceptualization.

Declaration of competing interest

The authors declare that they have no known competing financial interests or personal relationships that could have appeared to influence the work reported in this paper.

Data availability

No data was used for the research described in the article.

Appendix A. Bogoliubov's approximation

We briefly revisit the procedure that allows us to recast Hamiltonian (3) into a separable form [17]. To this end one must express Hamiltonian (1) in the momentum-mode picture by exploiting the relations (2) between the momentum modes a_k, b_k and space modes A_j, B_j with $j,k = 0,1,\ldots L-1$. The momentum-mode picture is very advantageous to describe the emergence of currents and vortex states involving intersite transport. The new Hamiltonian becomes

$$H = \frac{U_a}{2L}\sum_{k,p,q=0}^{L-1} a^\dagger_{q+k}a^\dagger_{p-k}a_q a_p - 2T_a\sum_{k=0}^{L-1} a^\dagger_k a_k\cos\tilde{k} + \frac{U_b}{2L}\sum_{k,p,q=0}^{L-1} b^\dagger_{q+k}b^\dagger_{p-k}b_q b_p - 2T_b\sum_{k=0}^{L-1} b^\dagger_k b_k\cos\tilde{k} + \frac{W}{L}\sum_{p,q,k=0}^{L-1} a^\dagger_{p+k}b^\dagger_{q-k}a_p b_q. \tag{A.1}$$

with $\tilde{k} = 2\pi k/L$. Within the Bogoliubov approximation, the condition that zero-momentum modes a_0 and b_0 are macroscopically occupied entails that

$$a^\dagger_0 a_0 \simeq N, \quad b^\dagger_0 b_0 \simeq M$$

(showing how the populations relevant to these number operators are much larger than the populations of the modes with $k \neq 0$). This allows one to recast four-operator terms such as

$$c^\dagger_{q+k}c^\dagger_{p-k}c_q c_p, \quad (c = a, b)$$

into a quadratic form that allows to implement the diagonalization process. The same simplification can be extended to the W-dependent term. The final form of Hamiltonian (A.1) for a L-site lattice, up to a constant term, reads $H = \text{const} + \sum_{k>0} H_k$ where

$$H_k = 2\gamma_{k,a}A_{3k} + 2\gamma_{k,b}B_{3k} + E_k + E_{-k}$$

and

$$E_{-k} = E_k^\dagger, \quad E_k = u_a A_k + u_b B_k + w(K_k + S_k),$$

with

$$A_k = a^\dagger_k a^\dagger_{-k}, \quad B_k = b^\dagger_k b^\dagger_{-k}, \quad A_{3k} = \frac{n_k + n_{-k} + 1}{2}, \quad B_{3k} = \frac{m_k + m_{-k} + 1}{2},$$

$$S_k = a^\dagger_k b_k + a^\dagger_{-k}b_{-k}, \quad K_k = a^\dagger_{-k}b^\dagger_k + a^\dagger_k b^\dagger_{-k},$$

and the number operators $n_k = a^\dagger_k a_k$, and $m_k = b^\dagger_k b_k$. The k-dependent Hamiltonian parameters are

$$\gamma_{ak} = u_a + 2T_a(1-\cos\tilde{k}), \quad \gamma_{bk} = u_b + 2T_b(1-\cos\tilde{k}), \tag{A.2}$$

while parameters u_a, u_b and w are given by Eq. (7). Such equations clearly show how parameters u_a, u_b and w bear memory of the Bogoliubov approximation due to their dependence on N and M, where N and M are the numbers associated to the macroscopic (conserved) populations of species a and species b, respectively. The implementation of this procedure for $L = 3$ brings us to find expression (3) where $\sum_{k>1} H_k = H_1$.

Appendix B. Dynamical algebra

In this section, we provide the commutation relations for the operators representing the generators of the dynamical algebra. These commutators allow one to verify that the set $\mathcal{A}$ constitutes a closed structure, namely a Lie algebra. The knowledge of the commutators is essential for implementing the dynamical-algebra method. Specifically, they are used to evaluate how unitary transformations act on operators by means of the Baker-Campbell-Hausdorff equation [41], [42],

$$e^{\hat{X}}\hat{Y}e^{-\hat{X}} = \sum_{s=0}^{\infty}\frac{1}{s!}[\hat{X},\hat{Y}]_s, \quad \hat{X},\hat{Y}\in\mathcal{A}. \tag{B.1}$$

This identity is fundamental for diagonalizing the Hamiltonian and for deriving the time evolution of the number operators. The ten generators of so(2,3) repeatedly exhibit the structure of algebra su(1,1). The three triplets of generators

$$A_1,\ A_2,\ A_3, \quad B_1,\ B_2,\ B_3, \quad K_1,\ K_2,\ K_3,$$

with $K_3 = A_3 + B_3$ satisfy the su(1,1) commutators

$$[C_2, C_1] = iC_3,\ [C_2, C_3] = iC_1,\ [C_3, C_1] = iC_2,$$

with $C = A, B, K$. On the other hand, the triplet S_1, S_2, $S_3 = A_3 - B_3$ features the su(2) commutators

$$[S_1, S_2] = iS_3,\ [S_2, S_3] = iS_1,\ [S_3, S_1] = iS_2.$$

Additionally, one finds vanishing commutators such as

$$[S_r, A_3 + B_3] = 0, \qquad [K_r, A_3 - B_3] = 0,$$

with $r = 1, 2$. At last, the commutator list of so(2,3) is completed by the mixed commutators

$$[A_1, S_1] = [B_1, S_1] = [A_2, S_2] = [S_2, B_2] = K_2/(2i),$$
$$[A_1, S_2] = [S_2, B_1] = [S_1, A_2] = [S_1, B_2] = K_1/(2i),$$
$$[A_1, K_1] = [K_1, B_1] = [A_2, K_2] = [K_2, B_2] = S_2/(2i),$$
$$[A_1, K_2] = [K_2, B_1] = [K_1, A_2] = [K_1, B_2] = S_1/(2i),$$
$$[S_1, K_1] = i(A_2 + B_2),\ [S_2, K_2] = -i(A_2 - B_2),$$
$$[S_1, K_2] = -i(A_1 + B_1),\ [S_2, K_1] = -i(A_1 - B_1).$$

Appendix C. The degenerate parametric amplifier

In this section, we revisit the dynamics of the degenerate parametric amplifier described by Hamiltonian [39]

$$H = \hbar w a^\dagger a + \hbar\gamma b^\dagger b + g\left(b^\dagger a^2 + a^{\dagger 2} b\right),$$

where w is the frequency of the photon mode described by a and $a^\dagger$, γ is the frequeny of the pump photon mode associated to b and $b^\dagger$, and the g-dependent interaction term describes the creation (destruction) of two a-mode photons due to the destruction (creation) of a b-mode photon. The resonance condition $2w = \gamma$ combined with the assumption that the pump mode is macroscopically occupied and therefore $b^\dagger b \simeq N_p >> 1$, with N_p the number of pump-mode photons, allows one to reduce Hamiltonian H to a simplified form

$$H_* = \hbar w a^\dagger a + v\left(a^2 + a^{\dagger 2}\right),$$

where the effective interaction parameter $v = g\sqrt{N_p}$ has been introduced. By resorting to the well-known two-photon realization of algebra su(1,1)

$$K_+ = \frac{1}{2}a^{\dagger 2}, \quad K_- = K_+^\dagger, \quad K_3 = \frac{1}{4}(2\hat{n} + 1), \tag{C.1}$$

where $K_1 = (K_+ + K_-)/2$, and $K_2 = -i(K_+ - K_-)/2$ satisfy the standard su(1,1) commutators $[K_3, K_\pm] = \pm K_\pm$, $[K_+, K_-] = -2K_3$ one gets

$$H_* = 2\hbar w K_3 + 4v K_1 - \hbar w/2. \tag{C.2}$$

showing K_3, the compact generator of su(1,1), and K_1, a non-compact generator together with K_2. Depending on the values of physical parameters, the diagonalization process can be realized by two independent transformations. In the physical regime $\hbar w > 2v$ (weak interaction) one has

$$e^{-i\mu K_2} K_3 e^{i\mu K_2} = K_3 \mathrm{ch}\mu + K_1 \mathrm{sh}\mu, \tag{C.3}$$

with $\mathrm{ch}\mu = \hbar w/R$, $\mathrm{sh}\mu = 2v/R$, and $R = \sqrt{\hbar^2 w^2 - 4v^2}$, whereas, in the opposite physical regime where $\hbar w < 2v$ (strong interaction), one has

$$e^{-i\nu K_2} K_1 e^{i\nu K_2} = K_1 \mathrm{ch}\nu + K_3 \mathrm{sh}\nu, \tag{C.4}$$

with $\mathrm{sh}\nu = \hbar w/r$, $\mathrm{ch}\nu = 2v/r$, and $r = \sqrt{4v^2 - \hbar^2 w^2}$. Then, one then finds, in the two cases, the Hamiltonians

$$H_d = -\frac{1}{2}\hbar w + 2\sqrt{\hbar^2 w^2 - 4v^2}\,K_3, \quad H_d' = -\frac{1}{2}\hbar w + 2\sqrt{4v^2 - \hbar^2 w^2}\,K_1,$$

where no amplification effect emerges from H_d due to the compact character of K_3, but crops up from H_d' due to the non-compact character of K_1. By using the Glauber coherent state $|z\rangle$ (defined by $a|z\rangle = z|z\rangle$) in the case $2v > \hbar w$, the calculation of the average photon number $\langle a^+ a\rangle$ shows, for $z \in \mathbb{R}$, the large-time diverging behavior

$$\langle a^+ a\rangle \simeq \frac{1}{4} e^{rt/\hbar}(2z^2 + 1)\mathrm{ch}\nu.$$

Note that the terms B_3 and B_1 in H_1 play the same role of operators K_3 and K_1 in the parametric-amplifier Hamiltonian (C.2). These simply represent a different two-boson mode realization of the su(1,1) generators. But the commutators of B_3, B_1, and B_2 (shown below formula (17)) coincide with the commutators for K_3, K_1, and K_2. The diagonalization of H_1 leads, in the instability case, to Hamiltonian (17) including B_1, the non-compact generator determining the amplification effect. This is same phenomenon described by H_d'.

References

[1] X.-Q. Xu, L.-H. Lu, Y.-Q. Li, Stability and dynamical property for two-species ultracold atoms in double wells, Phys. Rev. A 78 (2008) 043609.
[2] K.J.H. Law, P.G. Kevrekidis, L.S. Tuckerman, Stable vortex–bright-soliton structures in two-component Bose-Einstein condensates, Phys. Rev. Lett. 105 (2010) 160405.
[3] P. Kuopanportti, J.A.M. Huhtamaki, M. Möttonen, Exotic vortex lattices in two-species Bose-Einstein condensates, Phys. Rev. A 85 (2012) 043613.
[4] D. Spehner, L. Morales-Molina, S.A. Reyes, Persistent currents in Bose-Bose mixtures after an interspecies interaction quench, New J. Phys. 23 (2021) 063025.
[5] W.-C. Syu, D.-S. Lee, C.-Y. Lin, Regular and chaotic behavior of collective atomic motion in two-component Bose-Einstein condensates, Phys. Rev. A 101 (2020) 063622.
[6] C.-Y. Wang, Quantum echo in two-component Bose-Einstein condensates, Phys. Rev. A 109 (2024) 063327.
[7] A. Bellettini, A. Richaud, V. Penna, Massive-vortex realization of a Bosonic Josephson Junction, Phys. Rev. Res. 6 (2024) 043197.
[8] M.P.A. Fisher, P.B. Weichman, G. Grinstein, D.S. Fisher, Boson localization and the superfluid-insulator transition, Phys. Rev. B 40 (1989) 546.
[9] M. Hiller, T. Kottos, T. Geisel, Complexity in parametric Bose-Hubbard Hamiltonians and structural analysis of eigenstates, Phys. Rev. A 73 (2006) 061604.
[10] A.R. Kolovsky, Semiclassical Quantization of the Bogoliubov Spectrum, Phys. Rev. Lett. 99 (2007) 020401.
[11] A.I. Streltsov, K. Sakmann, O.E. Alon, L.S. Cederbaum, Accurate multi-boson long-time dynamics in triple-well periodic traps, Phys. Rev. A 83 (2011) 043604.
[12] E.R. Castro, K. Wittmann W., J. Chávez-Carlos, I. Roditi, A. Foerster, J.G. Hirsch, Quantum-classical correspondence in a triple-well bosonic model: From integrability to chaos, Phys. Rev. A 109 (2024) 032225.
[13] P. Buonsante, R. Franzosi, V. Penna, Dynamical Instability in a Trimeric Chain of Interacting Bose-Einstein Condensates, Phys. Rev. Lett. 90 (2003) 050404.
[14] S. Mossmann, C. Jung, Semiclassical approach to Bose-Einstein condensates in a triple well potential, Phys. Rev. A 74 (2006) 033601.
[15] F. Trimborn, D. Witthaut, H.J. Korsch, Beyond mean-field dynamics of small Bose-Hubbard systems based on the number-conserving phase-space approach, Phys. Rev. A 79 (2009) 013608.
[16] A.V. Varma, A. Vardi, D. Cohen, Characterization of hybrid quantum eigenstates in systems with mixed classical phase space, Phys. Rev. E 109 (2024) 064207.
[17] V. Penna, A. Richaud, Two-species boson mixture on a ring: a group-theoretic approach to the quantum dynamics of low-energy excitations, Phys. Rev. A 96 (2017) 053631.
[18] A. Brattley, T. Opatrny, K.K. Das, Spin-orbit and hyperfine simulations with two-species ultracold atoms in a ring, Phys. Rev. A 110 (2024) 023319.
[19] A. Richaud, V. Penna, Phase separation can be stronger than chaos, New J. Phys. 20 (2018) 105008.
[20] V. Penna, A. Contestabile, A. Richaud, Ground-state properties and phase separation of binary mixtures in mesoscopic ring lattices, Entropy 23 (2021) 821.
[21] M. Albiez, R. Gati, J. Fölling, S. Hunsmann, M. Cristiani, M.K. Oberthaler, Direct observation of tunneling and nonlinear self-trapping in a single Bosonic Josephson Junction, Phys. Rev. Lett. 95 (2005) 010402.
[22] G. Spagnolli, G. Semeghini, L. Masi, G. Ferioli, A. Trenkwalder, S. Coop, M. Landini, L. Pezzè, G. Modugno, M. Inguscio, A. Smerzi, M. Fattori, Crossing over from attractive to repulsive interactions in a tunneling bosonic Josephson junction, Phys. Rev. Lett. 118 (2017) 230403.
[23] L. Amico, A. Osterloh, F. Cataliotti, Quantum many particle systems in ring-shaped optical lattices, Phys. Rev. Lett. 95 (2005) 063201.
[24] D. Aghamalyan, L. Amico, L.C. Kwek, Effective dynamics of cold atoms flowing in two ring-shaped optical potentials with tunable tunneling, Phys. Rev. A 88 (2013) 063627.
[25] L. Amico, D. Anderson, M. Boshier, J.-P. Brantut, L.-C. Kwek, A. Minguzzi, W. von Klitzing, Colloquium: atomtronic circuits: from many-body physics to quantum technologies, Rev. Mod. Phys. 94 (2022) 041001.
[26] J. Catani, L. De Sarlo, G. Barontini, F. Minardi, M. Inguscio, Degenerate Bose-Bose mixture in a three-dimensional optical lattice, Phys. Rev. A 77 (2008) 011603(R).
[27] A. Burchianti, C. D'Errico, S. Rosi, A. Simoni, M. Modugno, C. Fort, F. Minardi, Dual-species Bose-Einstein condensate of 41 K and 87 Rb in a hybrid trap, Phys. Rev. A 98 (2018) 063616.
[28] K.L. Lee, N.B. Jørgensen, I. Kang Liu, L. Wacker, J.J. Arlt, N.P. Proukakis, Phase separation and dynamics of two-component Bose-Einstein condensates, Phys. Rev. A 94 (2016) 013602.
[29] G. Mazzarella, L. Salasnich, A. Parola, F. Toigo, Coherence and entanglement in the ground state of a bosonic Josephson junction: From macroscopic Schrödinger cat states to separable Fock states, Phys. Rev. A 83 (2011) 053607.
[30] A.I. Solomon, Group theory of superfluidity, J. Math. Phys. 12 (1971) 390.
[31] M. Rasetti, Generalized definition of coherent states and dynamical groups, Int. J. Theor. Phys. 13 (1975) 425.
[32] V. Penna, Dynamics of the central-depleted-well regime in the open Bose-Hubbard trimer, Phys. Rev. E 87 (2013) 052909.
[33] L. Duan, Y.-F. Xie, D. Braak, Q.-H. Chen, Two-photon Rabi model: analytic solutions and spectral collapse, J. Phys. A Math. Theor. 49 (2016) 464002.
[34] S. Felicetti, J.S. Pedernales, I.L. Egusquiza, G. Romero, L. Lamata, D. Braak, E. Solano, Spectral collapse via two-phonon interactions in trapped ions, Phys. Rev. A 92 (2015) 033817.
[35] G. Lindblad, B. Nagel, Continuous bases for unitary irreducible representations of SU(1,1), Ann. Inst. Henri Poincaré 13 (1970) 27.
[36] F. Lingua, M. Guglielmino, V. Penna, Demixing effects in mixtures of two bosonic species, Phys. Rev. A 92 (2015) 053610.

[37] W.M. Zhang, D.H. Feng, R. Gilmore, Coherent states: theory and some applications, Rev. Mod. Phys. 62 (1990) 867.
[38] V. Penna, F.A. Raffa, Dynamical properties of two coupled quantum cavities with single-mode amplification, Phys. Rev. E 110 (2024) 044126.
[39] M. Hillery, M.S. Zubairy, Path-integral approach to the quantum theory of the degenerate parametric amplifier, Phys. Rev. A 29 (1984) 1275.
[40] L. Mandel, E. Wolf, Optical Coherence and Quantum Optics, Cambridge University Press, Cambridge, 1995.
[41] R. Achilles, A. Bonfiglioli, The early proofs of the theorem of Campbell, Baker, Hausdorff, and Dynkin, Arch. Hist. Exact Sci. 66 (2012) 295.
[42] D. Martinez-Tibaduiza, A.H. Aragão, C. Farina, C.A.D. Zarro, New BCH-like relations of the su(1,1), su(2) and so(2,1) Lie algebras, Phys. Lett. A 384 (2020) 126937.